Mol. Cells *29*, 471-474, May 31, 2010
DOI/10.1007/s10059-010-0058-3

Molecules and Cells

Crystal Structures of Human FIH-1 in Complex with Quinol Family Inhibitors

Hyunjin Moon, Sojung Han, Hyunsung Park, and Jungwoo Choe*

Hypoxia-Inducible Factor-1 (HIF-1) plays an important role as a transcription factor under hypoxia. It activates numerous genes including those involved in angiogenesis, glucose metabolisms, cell proliferation and cell survival. The HIF-1α subunit is regulated by 2-oxoglutarate (OG)- and Fe(II)-dependent hydroxylases, including Factor Inhibiting HIF-1 (FIH-1). FIH-1 hydroxylates Asn803 of HIF-1α and blocks its interaction with co-activating molecules. Quinol family compounds such as 5-chloro-7-iodo-8-hydroxyquinoline (Clioquinol) have been shown to inhibit the hydroxylation activity of FIH-1. Here we determined the complex crystal structures of FIH-1: Clioquinol and FIH-1: 8-Hydroxyquinoline. Clioquinol and 8-Hydroxyquinoline bind to the active site of FIH-1 by coordinating the Fe(II) ion, thereby inhibiting the binding of a co-substrate, 2OG. Contrary to other known FIH-1 inhibitors that have negative charges, Clioquinol and 8-hydroxyquinoline are neutral in charge and can provide a template for improved inhibitor design that can selectively inhibit FIH-1.

INTRODUCTION

Mammalian cells have their own mechanism to survive under low oxygen concentration (hypoxia) by inducing several genes involved in angiogenesis, erythropoiesis, glycolysis, Fe(II) metabolism, vasodilation and cell survival (Lando et al., 2002). Most of these genes are activated by a heterodimeric transactivator, named hypoxia-inducible factor-1 (HIF-1). HIF-1 consists of α and β subunits which contain basic helix-loop-helix domain and Per-Arnt-Sim (PAS) domain in their N-termini (Wang et al., 1995). Under hypoxia, HIF-1α is stabilized and migrates from the cytoplasm to the nucleus and binds HIF-1β to form the activated heterodimer. HIF-1α/β heterodimer binds a specific DNA sequence located in enhancer regions of its target genes, then recruits a transcriptional co-activator, CREB binding protein (CBP) or p300 (the 300 KDa co-activator protein) through its C-terminal activation domain (CAD)(Arany et al., 1996).

The activity or the stability of HIF-1α is regulated by two distinct hydroxylases, HIF-1α prolyl hydroxylase (PHD) and asparaginyl hydroxylases, named Factor inhibiting HIF-1 (FIH-1) (Berra et al., 2003; Hewitson et al., 2002). Both of them belong to the 2OG (oxoglutarate)- and Fe(II)- dependent dioxygenase superfamily (Dann et al., 2002; Elkins et al., 2003). Because their hydroxylation activities are dependent on the level of molecular oxygen in the cell they are considered as cellular oxygen sensors (Schofield and Ratcliffe, 2004). FIH-1 hydroxylates the Asn803 of HIF-1α in normoxia, using oxygen and 2OG as a co-substrate, producing carbon dioxide and succinate as byproducts (Schofield and Zhang, 1999). This hydroxylation blocks HIF-1α from recruiting CBP or p300, thereby preventing the transcriptional activation of its target genes (Kung et al., 2004). Considering the pathophysiological importance of HIF-1α target genes, FIH-1 can be a molecular target for developing new therapeutic agents for conditions like cancer or cardiovascular diseases (Hewitson et al., 2004).

Structural studies of FIH-1 have shown that it forms a homodimer, and each subunit has a double-stranded β-helix core, a jellyroll-like-barrel which embraces the conserved active site with bound Fe(II). These features are shared by the 2OG dependent dioxygenase superfamily (Dann et al., 2002). Although structures of FIH-1 with bound inhibitors including *N*-oxalylglycine (NOG) (Elkins et al., 2003), tricarboxylic acid intermediates such as fumarate and succinate (Hewitson et al., 2007) and N-oxalyl amino acid (McDonough et al., 2005) were previously determined, it is questionable whether these compounds can be used for medicinal applications. The above mentioned inhibitors contain one or two carboxylate groups with substantial negative charges (-1~-2), which may impair their use as therapeutic agents. NOG is also known to inhibit other 2OG oxygenases, such as procollagen prolyl hydroxylase or phytanoyl Co-A hydroxylase (McDonough et al., 2005). Clioquinol, a Zn(II)/Cu(II) chelator, was shown to stabilize the transactive HIF-1α by blocking both Asn-hydroxyation and ubiquitination (Choi et al., 2006). Therefore, we have focused on quinol family compounds, such as 5-chloro-7-iodo-8-hydroxyquinoline (CQ, Clioquinol) and 8-Hydroxyquinoline (HQ), which are neutral in charge. Here we present the complex structures of FIH-1 with bound CQ and HQ and suggest possible modifications for improved inhibitor design.

MATERIALS AND METHODS

Protein expression and purification

The cloning and expression of full-length human FIH-1 (residue

Department of Life Science, University of Seoul, Seoul 130-743, Korea
*Correspondence: jchoe@uos.ac.kr

Received November 10, 2009; revised January 14, 2010; accepted February 10, 2010; published online April 12, 2010

Keywords: clioquinol, crystal structure, factor Inhibiting HIF-1 (FIH-1), hypoxia, hypoxia-inducible factor-1 (HIF-1)

Table. 1. Data collection and refinement statistics

Crystals	FIH-1: CQ (Clioquinol)	FIH-1: HQ (8-Hydroxyquinoline)
X-ray Source	PAL-4 A	PAL-6C1
Space Group	$P4_12_12$	$P4_12_12$
Unit Cell Dimensions (Å)	a = 86.746 b = 86.746 c = 146.525	a = 86.9 b = 86.9 c = 144.56
Resolution (Å)	20-2.6 (2.64-2.60)	20-2.6 (2.64-2.60)
Observed Reflections	1,182,407	248,296
Unique Reflections	17,839	17,618
Completeness (%)	100 (100)	99.9 (100)
R_{symm}[1] (%)	10.7 (59.5)	6.9 (57.4)
I / σ (I)	22.9 (4.0)	30.6 (3.7)
Refinement statistics		
Resolution (Å)	20-2.6 (2.64-2.60)	20-2.6 (2.64-2.60)
No. of Residues	332	332
R_{cryst}[2] (%)	23.88	23.23
R_{free}[3] (%)	28.33	30.75
RMSD bond Length (Å)	0.017	0.018
RMSD bond Angle (°)	1.787	1.742

Numbers in parentheses on the right indicate the statistics for the highest resolution shell

[1] $R_{symm} = \sum_{hkl} \sum_i |I_i(hkl) - \langle I(hkl) \rangle| / \sum_{hkl} \sum_i I_i(hkl)$

[2] R_{cryst} (%) = $\sum$ |Fo-Fc| / $\sum$ Fo

[3] R_{free} (%) is calculated in the same manner as R_{cryst} using 5% of reflections excluded from refinement.

1-349) have been described previously (Lee et al., 2003). Briefly, the recombinant FIH-1 protein cloned in the pET28a vector (Novagen), with an N-terminal His_6-tag, was overexpressed using BL21(DE3) *E. coli* strain (Novagen). The cells were lysed by sonication on ice in 50 mM NaPhosphate pH 7.0 with 200 mM NaCl. The protein was first purified by the Ni-NTA affinity column (GE healthcare) and then the N-terminal His_6-tag was digested with thrombin. The protein was then applied to a Superdex 75 column equilibrated with 10 mM Tris-HCl pH 7.5, 200 mM NaCl, 2 mM DTT and 2 mM EDTA. Fractions containing FIH-1 was confirmed by SDS-PAGE and concentrated to a final concentration of 9 mg ml^{-1} using a centrifugal filter device (Amicon Ultra-4 Centrifugal Filters (NMWL 10,000) from Millipore).

Crystallization

All crystallization trials were performed using the hanging-drop vapor-diffusion method by mixing equal volumes (1.0 μl) of the protein and reservoir solutions and equilibrating the mixed solutions against a 500 μl reservoir solution, in a 24-well plate at 20°C. Crystals of FIH-1 in complex with both CQ and HQ grew, using a reservoir solution with 1.6 M ammonium sulfate, 2% polyethyleneglycol 400 and 0.1 M Tris-HCl pH 7.5. Due to the limited solubility of CQ in H_2O, the protein solution for FIH-1: CQ complex was prepared by mixing 48 μl 9.0 mg ml^{-1} FIH-1 with 5.0 μl 0.5 M CAPS pH 11.0, 5.0 μl 100% DMSO, 1.0 μl 200 mM $(NH_4)_2Fe(SO_4)_26H_2O$ and 1.0 μl 200 mM CQ dissolved in DMSO. The protein solution for FIH-1: HQ complex was made by mixing 48 μl 9.0 mg ml^{-1} FIH-1 with 1.0 μl 200 mM $(NH_4)_2Fe(SO_4)_26H_2O$ and 5.0 μl 200 mM HQ dissolved in ethanol. It took about 4 weeks for the crystals to grow to their full size.

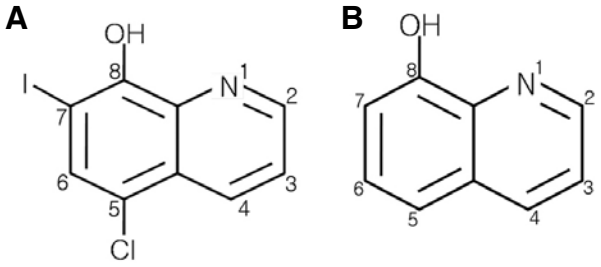

Fig. 1. Chemical structures of (A) 5-chloro-7-iodo-8-hydroxyquinoline (Clioquinol, CQ) and (B) 8-Hydroxyquinoline (HQ).

The cryoprotectant solution was made by adding 30% glycerol to the reservoir solution and added gradually to the crystals in order to minimize the deterioration of diffraction quality.

Data collection and structure determination

Crystals in a cryoprotectant solution was flash-frozen in liquid N_2. The data were collected in 6C and 4A beamline of Pohang Accelerator Laboratory (PAL, KOREA). Data were processed and scaled with HKL-2000 program. Both the FIH-1: CQ and FIH-1: HQ crystals belonged to a space group $P4_12_12$ with cell dimensions shown in table 1. Assuming one molecule of FIH-1 in the asymmetric unit, the Matthews coefficient is 3.4 $Å^3 Da^{-1}$. The structures of the FIH-1: CQ and FIH-1: HQ complexes were solved by molecular replacement, using the MOLREP program, with the apo FIH-1 structure as a model (Vagin and Teplyakov, 2000). The structures were refined with rigid-body and restraint refinement protocol of the REFMAC program (Murshudov et al., 1997). Manual model building and adjustments were performed using the program Coot (Emsley and Cowtan, 2004). The Ramachandran plot calculated with the program PROCHECK showed no residues in the disallowed region. The data collection and the refinement statistics are summarized in Table 1. Atomic coordinates have been deposited to the Protein Data Bank under accession codes 3KCX and 3KCY.

RESULTS AND DISCUSSION

Complex structures of FIH-1 with CQ and HQ

CQ and HQ both belong to the drug family hydroxyquinolines (Fig. 1). To further investigate the inhibitory mechanism of CQ that inhibits the hydroxylation of HIF-1α by FIH-1, we determined the crystal structures of FIH-1 with CQ and its parent compound HQ. Complex structures of FIH-1: CQ and FIH-1: HQ showed very similar overall structural features to the previously determined FIH-1 structures (Dann et al., 2002): the central core is composed of a β-barrel surrounded by eight α-helices, where an active site pocket is located. Together with 2OG, residues including His199, Asp201, and His279 coordinate Fe(II) in the active site (Fig. 2C) and these residues are called the 2-His-1-carboxylate facial triad. CQ and HQ bind in the active site of FIH-1 and occupy a position that can replace the cosubstrate, 2OG (Fig. 2). Instead of 2OG, CQ and HQ participate in the coordination of Fe(II), using the oxygen in the 8-hydroxyl group and 1-nitrogen atom in the quinoline ring, which are present in both compounds. The distances between Fe(II) and the coordinating atoms range from 2.0 to 2.5 Å. CQ and HQ also interact with nearby residues in the active site, such as Gln147, Leu186, Leu188, Phe207, Ile273, His279, Ile281, and Trp296 for mainly hydrophobic interactions (Fig. 2). Thus two factors contribute to the binding affinity of CQ: The

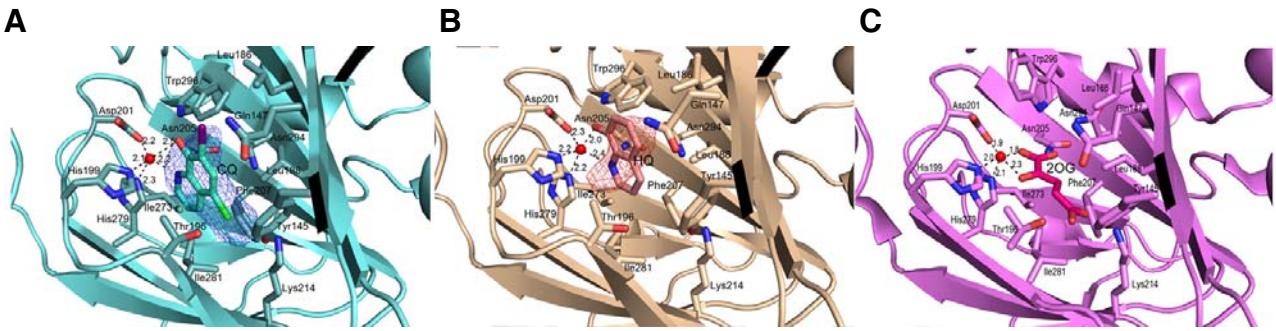

Fig. 2. Binding mode of inhibitors and cosubstrate. Residues involved in Fe(II) coordination or inhibitor/cosubstrate binding in the active site of FIH-1 are shown. The distances between Fe(II) and coordinating atoms are indicated. (A) The binding mode of CQ and (B) 8-HQ with initial F_O-F_C difference electron density drawn at a contour level of 2.4σ. (C) The binding mode of 2OG (PDB ID: 1H2N). Oxygens are colored in red, nitrogens in blue, iodine in purple and chlorine in green, respectively.

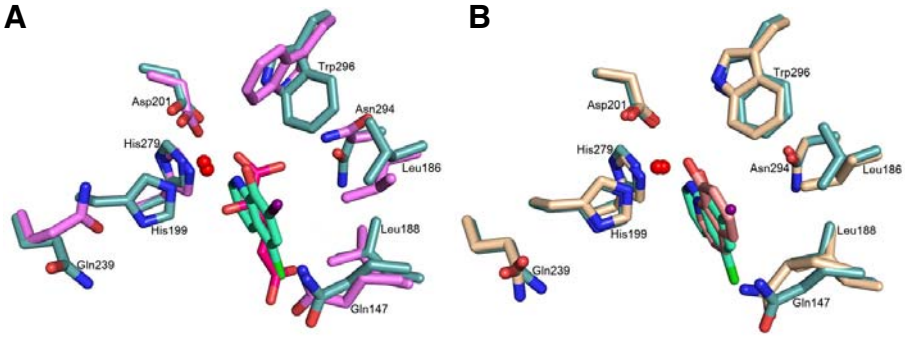

Fig. 3. Comparison of binding modes and conformational changes upon inhibitor binding. (A) Superposition of CQ and 2OG. Residues that show significant conformational changes are drawn together with Fe(II) and three coordinating residues (His199, Asp201 and His279). The coloring scheme is same as Fig. 2. The carbons of CQ are colored in green and 2OG in pink. (B) Superposition of CQ and HQ complex structures shows their coplanar binding mode. The carbons of CQ are colored in green and HQ in orange.

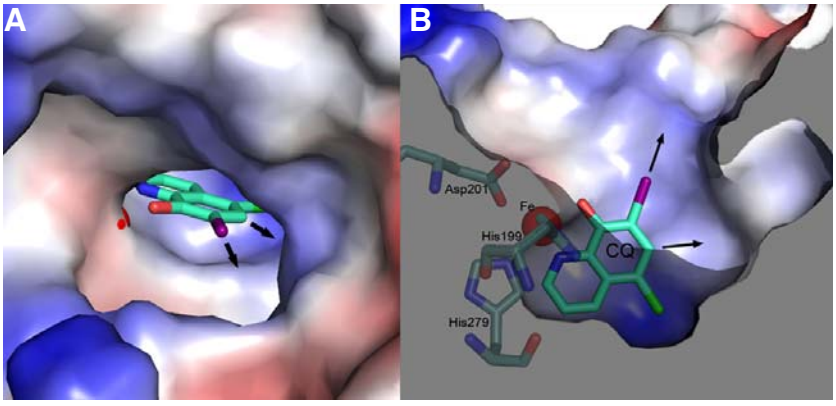

Fig. 4. Surface representation of the FIH-1 active site colored with electrostatic potential. (A) CQ drawn in stick is shown inside the active site coordinating the ferrous ion (red). The iodine (purple) at position 7 is pointing towards the opening of the pocket. (B) The view is rotated about 90° along the x-axis from (A). The grey area represents the inside of the protein. Three residues coordinating Fe(II) ion are also shown. The positions available for chemical modifications are indicated by arrows.

coordination of Fe(II) with 8-hydroxyl group and 1-nitrogen atom as well as hydrophobic interactions between halogenated quinoline ring and the surrounding residues. HQ does not have halogens such as iodine and chlorine which are present in CQ and is believed to be a weaker inhibitor of FIH-1. This is also reflected by the weaker electron density of HQ compared to CQ (Fig 2).

Comparison of binding modes of inhibitors and substrate

The binding modes of CQ and HQ partially overlap with that of 2OG and thus may explain their function as a competitive inhibitor (Fig. 3). Although the inhibitors (CQ and HQ) and the cosubstrate 2OG all coordinate Fe(II) in the active site of FIH-1, the binding modes of inhibitors are quite different from 2OG (Fig. 2). For example, the 1-nitrogen and 8-hydroxyl groups of CQ/HQ that coordinate Fe(II) are almost perpendicular to the two oxygen atoms of 2OG, which are involved in Fe(II) coordination. Also, the residues around CQ (Gln147, Leu186, Asn294, Trp296) rearranged, making the binding pocket bigger compared to that of the 2OG structure (Fig. 3A). This is partly due to the larger size of iodine in CQ, and a longer interaction distance between iodine and Leu186. Trp296 rotates about 90° to make contacts with the iodine, the ring carbons of CQ and Leu186. Asn294 that used to form a hydrogen bond with the cosubstrate 2OG, cannot form a hydrogen bond with CQ and thus is now free to move, to optimize the Van der Waals interaction with Leu188. Gln147, which interacts with the chlorine atom of CQ, also moves about 1.1 Å away from CQ. The superposition of the CQ and HQ complex structures shows that the quinoline rings of these two inhibitors are along the same plane (Fig. 3B).

However, the quinoline ring of CQ and HQ does not overlap completely, and CQ occupies a deeper position in the pocket. In the case of HQ, rearrangements observed in the FIH-1: CQ structure are also observed, except Leu186, which did not move due to the absence of iodine (Fig. 3B).

Prospects for improved inhibitor design

CQ was once a widely used oral antiparasitic especially in Japan to treat indigestion and diarrhea. However, it was banned when it was reported to cause a serious side effect called Subacute Myelo-Optic-Neuropathy (SMON), a neurodegenerative disorder that leads to paralysis and blindness (Tabira, 2001; Tateishi, 2000). But the causal relationship between CQ and SMON has never been proven (Bush and Masters, 2001). Recent findings have shown that CQ, functioning as a metal chelator, can be used to treat neurodegenerative diseases like Alzheimer's and Huntington's with controlled dosing and vitamin supplementation (Nguyen et al., 2005; Raman et al., 2005; Ritchie et al., 2003). Although the mechanism of action of CQ against these neurodegenerative diseases probably involves the chelation of free metal ions (which is different from the inhibition mechanism of FIH-1, where CQ replaces one of the substrate), the use of Clioquinol to treat these conditions represents the bioavailability and low cytotoxicity of CQ.

We examined the possibility of CQ modifications to achieve higher selectivity and affinity of CQ derivatives. Surface representation of FIH-1 shows that CQ binds deep inside the binding pocket (Fig. 4A). With the binding mode of CQ observed in our crystal structure, 8-hydroxyl and 1-nitrogen of CQ are involved in coordinating the Fe(II) ion, and the other positions (2, 3, 4 and 5-positions, see Fig. 1 for numbering) are buried in the pocket and cannot accommodate other functional groups (Fig. 4B). 7-iodine and 6-carbon positions are, on the other hand, facing outward to the surface or space inside the pocket, and they provide opportunities for chemical modifications. Comparisons with other structurally homologous proteins that share similar domain structures with FIH-1 revealed that there are differences in the shape and surface charge distribution around the active site. From the observed binding mode of CQ in FIH-1, we propose that CQ can be modified to improve the specificity of CQ derivatives, without losing the ability to coordinate Fe(II) which is an important factor in maintaining the binding affinity.

ACKNOWLEDGMENTS

We thank the staff members of beamline 4A and 6C at the Pohang Accelerator Laboratory, Pohang, Korea. This work was supported by the Korea Science and Engineering Foundation grant, funded by the Korea government (MOST, R01-2007-000-10874-0).

REFERENCES

Arany, Z., Huang, L., Eckner, R., Bhattacharya, S., Jiang, C., Goldberg, M., Bunn, H., and Livingston, D. (1996). An essential role for p300/CBP in the cellular response to hypoxia. Proc. Natl. Acad. Sci. USA *93*, 12969.

Berra, E., Benizri, E., Ginouves, A., Volmat, V., Roux, D., and Pouyssegur, J. (2003) HIF prolyl-hydroxylase 2 is the key oxygen sensor setting low steady-state levels of HIF-1alpha in normoxia. EMBO J. *22*, 4082.

Bush, A., and Masters, C. (2001). Clioquinol's return. Science *292*, 2251-2252.

Choi, S., Choi, K., Park, Y., Cho, H., Yang, E., and Park, H. (2006). Clioquinol, a Cu (II)/Zn (II) chelator, inhibits both ubiquitination and asparagine hydroxylation of hypoxia-inducible factor-1 {alpha}, leading to expression of vascular endothelial growth factor and erythropoietin in normoxic cells. J. Biol. Chem. *281*, 34056.

Dann, C.E., 3rd, Bruick, R.K., and Deisenhofer, J. (2002). Structure of factor-inhibiting hypoxia-inducible factor 1: An asparaginyl hydroxylase involved in the hypoxic response pathway. Proc. Natl. Acad. Sci. USA *99*, 15351-15356.

Elkins, J.M., Hewitson, K.S., McNeill, L.A., Seibel, J.F., Schlemminger, I., Pugh, C.W., Ratcliffe, P.J., and Schofield, C.J. (2003). Structure of factor-inhibiting hypoxia-inducible factor (HIF) reveals mechanism of oxidative modification of HIF-1 alpha. J. Biol. Chem. *278*, 1802-1806.

Emsley, P., and Cowtan, K. (2004). Coot: model-building tools for molecular graphics. Acta Crystallogr. Section D: Biol. Crystallogr. *60*, 2126-2132.

Hewitson, K.S., McNeill, L.A., Riordan, M.V., Tian, Y.M., Bullock, A.N., Welford, R.W., Elkins, J.M., Oldham, N.J., Bhattacharya, S., Gleadle, J.M., et al. (2002). Hypoxia-inducible factor (HIF) asparagine hydroxylase is identical to factor inhibiting HIF (FIH) and is related to the cupin structural family. J. Biol. Chem. *277*, 26351-26355.

Hewitson, K.S., McNeill, L.A., and Schofield, C.J. (2004). Modulating the hypoxia-inducible factor signaling pathway: applications from cardiovascular disease to cancer. Curr. Pharm. Des. *10*, 821-833.

Hewitson, K.S., Lienard, B.M., McDonough, M.A., Clifton, I.J., Butler, D., Soares, A.S., Oldham, N.J., McNeill, L.A., and Schofield, C.J. (2007). Structural and mechanistic studies on the inhibition of the hypoxia-inducible transcription factor hydroxylases by tricarboxylic acid cycle intermediates. J. Biol. Chem. *282*, 3293-3301.

Holm, L., and Sander, C. (1995). Dali: a network tool for protein structure comparison. Trends Biochem. Sci. *20*, 478-480.

Kung, A., Zabludoff, S., France, D., Freedman, S., Tanner, E., Vieira, A., Cornell-Kennon, S., Lee, J., Wang, B., and Wang, J. (2004). Small molecule blockade of transcriptional coactivation of the hypoxia-inducible factor pathway. Cancer Cell *6*, 33-43.

Lando, D., Peet, D.J., Gorman, J.J., Whelan, D.A., Whitelaw, M.L., and Bruick, R.K. (2002). FIH-1 is an asparaginyl hydroxylase enzyme that regulates the transcriptional activity of hypoxia-inducible factor. Genes Dev. *16*, 1466-1471.

Lee, C., Kim, S., Jeong, D., Lee, S., and Ryu, S. (2003). Structure of human FIH-1 reveals a unique active site pocket and interaction sites for HIF-1 and von Hippel-Lindau. J. Biol. Chem. *278*, 7558-7563.

McDonough, M.A., McNeill, L.A., Tilliet, M., Papamicael, C.A., Chen, Q.Y., Banerji, B., Hewitson, K.S., and Schofield, C.J. (2005). Selective inhibition of factor inhibiting hypoxia-inducible factor. J. Am. Chem. Soc. *127*, 7680-7681.

Murshudov, G.N., Vagin, A.A., and Dodson, E.J. (1997). Refinement of macromolecular structures by the maximum-likelihood method. Acta Crystallogr. D. Biol. Crystallogr. *53*, 240-255.

Nguyen, T., Hamby, A., and Massa, S.M. (2005). Clioquinol down-regulates mutant huntingtin expression in vitro and mitigates pathology in a Huntington's disease mouse model. Proc. Natl. Acad. Sci. USA *102*, 11840-11845.

Raman, B., Ban, T., Yamaguchi, K., Sakai, M., Kawai, T., Naiki, H., and Goto, Y. (2005). Metal ion-dependent effects of clioquinol on the fibril growth of an amyloid {beta} peptide. J. Biol. Chem. *280*, 16157.

Ritchie, C., Bush, A., Mackinnon, A., Macfarlane, S., Mastwyk, M., MacGregor, L., Kiers, L., Cherny, R., Li, Q., and Tammer, A. (2003). Metal-protein attenuation with iodochlorhydroxyquin (clioquinol) targeting abeta amyloid deposition and toxicity in Alzheimer disease A pilot phase 2 clinical trial. Vol. 60, (Am. Med. Assoc.), pp. 1685-1691.

Schofield, C., and Ratcliffe, P. (2004). Oxygen sensing by HIF hydroxylases. Nat. Rev. Mol. Cell Biol. *5*, 343-354.

Schofield, C., and Zhang, Z. (1999). Structural and mechanistic studies on 2-oxoglutarate-dependent oxygenases and related enzymes. Curr. Opin. Struct. Biol. *9*, 722-731.

Tabira, T. (2001). Clioquinol's return: cautions from Japan. Science *292*, 2251.

Tateishi, J. (2000). Subacute myelo-optico-neuropathy: clioquinol intoxication in humans and animals. Neuropathology *20*, 20-24.

Vagin, A., and Teplyakov, A. (2000). An approach to multi-copy search in molecular replacement. Acta Crystallogr. Section D: Biol. Crystallogr. *56*, 1622-1624.

Wang, G., Jiang, B., Rue, E., and Semenza, G. (1995). Hypoxia-Inducible Factor 1 is a Basic-Helix-Loop-Helix-PAS Heterodimer Regulated by Cellular O SUB 2/SUB Tension. Proc. Natl. Acad. Sci. USA *92*, 5510-5514.